Entropy Multi-Objective Evolutionary Algorithm for Oil Spill Detection from RADARSAT-2 Data

M. Marghany

Institute of Geospatial Science and Technology (INSTeG), Universiti Teknologi Malaysia,
81310 UTM, Skudai, Johor Bahru, Malaysia
maged@utm.my

Abstract – *This study has demonstrated a design tool for oil spill detection in SAR satellite data using optimization of Entropy based Multi-Objective Evolutionary Algorithm (E-MMGA) based on Pareto optimal solutions. The study also shows that optimization entropy based on Multi-Objective Evolutionary Algorithm provides an accurate pattern of oil slick in SAR data. This is shown by 85% for oil spill, 10% look–alike and 5% for sea roughness using the receiver –operational characteristics (ROC) curve. The E-MMGA also shows excellent performance in SAR data. In conclusion, E-MMGA can be used as optimization for entropy to perform an automatic detection of oil spill in SAR satellite data.* **Copyright © 2015 Penerbit Akademia Baru - All rights reserved.**

Keywords: Entropy, Multi-Objective Evolutionary Algorithm, RADARSAT-2 SAR, oil spill, Pareto optimal solutions, Automatic detection

1.0 INTRODUCTION

Lately, oil spills in coastal zones have received much critical anxiety for the great damages on the coastal ecological system. Synthetic aperture radar (SAR) is proved as appropriate sensors for oil spill surveying for its wide-area and all-day all-weather surveillance potentials. Owing to its extraordinary imaging mechanism, conversely, the accuracy of oil spill detection is challenged by multiplicative speckle noise and dark patches instigated by other physical phenomena. In this perspective, dark patches not related to oil spills are known as look-alikes. They can be recognized to zones of low wind speed, internal waves, biogenic films, grease ice, wind front areas, areas sheltered by land, rain cells, current shear zones and up-welling zones [1]. Besides, three steps are expected to automatically detect oil spills in SAR images: (i) dark spot detection, (ii) dark spot feature extraction and (iii) dark spot classification. Various classification algorithms for oil spill detection have been utilized, including pattern recognition algorithms [3], spatial frequency spectrum gradient algorithms [1, 4] and algorithms based on fuzzy and neural networks [5, 6]. Consequently, oil spill automatic detection from SAR data requested standard algorithm to overwhelm the multiplicative speckle noise and look-alike phenomena effects.

Entropy algorithm was implemented to generate accurate assessment of the optimal oil spill monitoring in SAR data. The entropy algorithm considers the discrimination between oil spill footprint and look-alikes in SAR data. Therefore, the algorithm can support the automatic detection of oil spill by reducing uncertainty on the basis of information produced by multiplicative speckle noise and look-alike phenomena effects. In this regard, Marghany [2]

introduced entropy as accurate algorithm for oil spill automatic detection in SAR images. Further, Shi et al. [7] implemented entropy texture algorithm for oil spill detection from SAR and optical remote sensing. They found that the oil spill pixels are smoother than the surrounding environment. In fact, entropy algorithm reduces the multiplicative noise from oil spill pixels.

Conversely, Skrunes et al., [8] reported several disadvantages associated with oil spill detection using the current SAR sensors and stated that SAR sensors cannot detect the thickness distribution, volume, oil/water emulsion ratio or chemical properties of an oil slick. Instead, they recommended the use of multi-polarization observations, i.e., the data acquired by the RADARSAT-2 and TerraSAR-X satellites. Minchew et al., [9] stated that the comparison of entropy with aerial observations indicates that the variability of the entropy was consistent with the variability of the oil properties suggesting that the entropy provides a qualitative measure of the oil characteristics. Specifically, when there are open water and a thin sheen, the entropy is close to 0, but in the presence of thicker oil (e.g. emulsion) the entropy has values that are close to 1. In addition, quad-pol RADARSAT-2 SAR can provide information about oil spill thickness compared to other SAR single channel such as RADARSAT-1 SAR, ERS-1/2 and Terra SAR.

Furthermore, these researchers demonstrated that multi-polarization data could accurately discriminate between mineral oil slicks and biogenic slicks. Incidentally, Cloude and Pottier [10] introduced the Cloude-Pottier entropy algorithm (H) ($0 \leq H \leq 1$) which provides a measure of the amount of mixing between scattering mechanisms. For a wind-roughened ocean surface, the scattering is dominated by a single dominant scattering mechanism, namely Bragg scattering (H → 0). In the presence of an oil slick, however, the entropy increases (H→ 1) which is due to the increasing number of independent scattering mechanisms due to the damping of the small-scale Bragg waves. Nevertheless, in the region between imaging slick-free water and an oil slick, the entropy varied as a function of the properties of the oil (e.g. sheen, emulsion).

Recently, Staples and Touzi [11] stated that the entropy cannot be obtained from single co-polarized radar data, but requires quad-polarized data. Quad-polarized data means that the radar acquires two co-polarized channels (HH and VV) and two cross-polarized channels (HV and VH), but equally as important; quad-polarized data are phase-preserving meaning that the inter-channel phase difference (e.g. phase difference between HH and VV) is available. In contrast, Marghany [2] and Marghany and Genderen [12] claimed that entropy texture algorithm provides excellent performance for oil spill automatic detection from different single SAR data.

Recently, Marghany (2014) utilized the Genetic algorithm (GA) as automatic detection algorithm for oil spill in RADARSAT-2 SAR data. Marghany [2] confirmed the work of Topouzelis et al. [13]. Both studies agreed that the genetic algorithm was able to extract oil spill footprint boundaries automatically from the surrounding pixels without using a separate segmentation algorithm, as was done by Skrunes et al. [8]. Consistent with Marghany [16], the genetic algorithm has the ability to determine the optimal number of regions of oil spill segmentation or to choose certain features, i.e., the size of the analysis window or selected heuristic thresholds. Furthermore, the GA is shown to be able to identify and remove pixels that do not significantly contribute to oil slick footprint in SAR data. This conclusion has approved the findings of Mohanta and Sethi [15].

The novelty of this work is in the designing of the optimization tool for the real time oil spill automatic detection using Entropy-Based Multi-objective Evolutionary Algorithm without involving other tools such as neural network or any image processing classification tools. Indeed, previous studies have executed artificial neural networks [15, 16] or post-classification techniques [2], which are considered to be semi-automatic techniques. Furthermore, both artificial neural networks and post-classification techniques are time-consuming and the probability of misclassification does not always decrease as the number of features increases, especially when the sample data are insufficient.

Incidentally, the main objective of this work is to minimalize the look-alike dark pixels for accurate oil spill automatic detection in SAR satellite data which could be involved with oil spill footprint detected by entropy and genetic algorithm. The Entropy-Based Multi-objective Evolutionary Algorithm uses both basic and advanced operators. For illustrative purposes, the method has been operated onto oil spill footprint boundary shape optimization which allows local and global optimizations. Indeed, global optimization involves finding the optimal oil spill boundary shapes in SAR images. Look-alike pixels can be removed to reach the optimal oil spill automatic shape detection.

2.0 METHODOLOGY

2.1 Data Set

In this study, RADARSAT-2 SAR data acquired by RADARSAT-2 operating in ScanSAR Narrow single beam mode on April 27th, 2010 are investigated for oil spill detection in the Gulf of Mexico (Figure 1). The ScanSAR mode provides images with very wide swaths in single pass of the satellite. In addition, ScanSAR data can be produced either with a single linear co-polarization, or with a single linear cross- polarization or with dual co- and cross-polarization. The satellite is equipped with synthetic aperture radar (SAR) with multiple polarisation modes, including a fully polarimetric mode in which HH, HH, VV and VH polarised data are acquired [24].
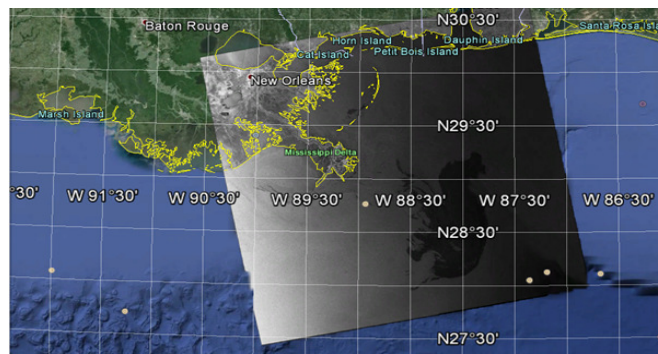
Figure 1: ScanSAR RADASAT-2 SAR of Deepwater Horizon Blowout, Gulf of Mexico.

2.2 Entropy-Based Multi-objective Evolutionary Algorithm (E-MMGA)

Two methods are involved to perform oil spill identification from RADARSAT-2 SAR (i) Entropy; and (ii) Entropy-Based Multi-objective Evolutionary Algorithm (E-MMGA).

2.2.1 Entropy Algorithm

Following Harmancioglu [17], entropy is a quantitative computation of the information content of a series of data since the reduction of uncertainty, by making observations, equals the same amount of gain in information. Therefore, Marghany [2] stated that entropy is a measure of the degree of uncertainty of random oil spill footprint discrimination [12]. In a definition adopted from information theory [28], entropy is the numerical expression of oil spill footprint boundaries in SAR images. In using this concept, oil spill footprint can be measured indirectly based on the degree of the reduction of multiplicative speckle noises and uncertainty of look-alike effects. The main hypothesis is the oil spill footprint boundaries have larger entropy compared to the surrounding environment. Hence, in order to quantitatively assess the cumulative effect of uncertainty in oil spill footprint, entropy can be used as a metric for population diversity of oil spill footprint boundaries which are stored at each intersection of the column j and row i of the various slick areas. The uncertainty (C) associated with the oil spill pixel value of x_i for a random variable X is given by [28]:

$$C(x_i) = \ln(p(x_i))^{-1} \tag{1}$$

where p_i is the probability distribution of $X_1 = \{x_i\}$ and i is represented raw. The expected value of all of the entropy (E) correlated with the random variable X is given by the following expression:

$$E(X) = \sum_i p(x_i) \ln(p(x_i))^{-1} \tag{2}$$

Equations 1 and 2 express the probability of oil spill footprint boundaries and their entropy in raw i. Therefore, Eq. 2 can be given in two directions of raw i and column j, then the two dimensional entropies $E(X,Y)$ are given as

$$E(X,Y) = \sum_j \left[\sum_i p(x_i, y_j) \ln(p(x_i, y_j))^{-1} \right] \tag{3}$$

Equation 3, in other words, represents the joint uncertainty associated with oil spill footprint boundaries in two dimensional of SAR images. It is assumed that the random variables of oil spill and look-alikes footprint boundaries are independent then equation 3 can be extended as

$$E(X,Y) = \sum_j \left[\sum_i p(x_i) p(y_j) \ln(p(x_i)^{-1} p(y_j)^{-1}) \right] \tag{4}$$

Equation 4 can be extended to an n-dimensional vector of independently distributed of oil spill and look-alikes footprint boundaries random variables in SAR data. Hence, in this case, the entropy $E(Z)$ is the sum of all of the individual SAR pixel entropies $E(X_i)$ and can be expressed as

$$E(Z) = \sum_j^n E(X_i) \tag{5}$$

In the case of a uniform distribution of given oil spill or look-alikes footprint boundaries, the entropy of given probability $p(x_i)=N^{-1}$ of the number (N) of homogenous clustering of the features can be calculated as

$$E(Z) = \sum_{i=1}^{N} \frac{\ln(N)}{N} \tag{6}$$

The number of features (n) in the SAR image space solution can be estimated based on the upper bound on the joint entropy $E_u(Z)$ for oil spill or look-alikes footprint boundary population as

$$E_u(Z) = n\ln(N) \tag{7}$$

Based on Equations 6 and 7 the entropy metric is bounded by

$$0 \le E(Z) \le E_u(Z) \tag{8}$$

Based on Equation 8, the final entropy metric expression can be written by the combination of equations 6 and 7 as follows:

$$0 \le \sum_{j=1}^{n}\left[\sum_{i=1}^{N} p(\beta_{i,j})\ln\left(p(\beta_{i,j})^{-1}\right)\right] \le n\ln(N) \tag{9}$$

where $p(\beta_{i,j})$ is the probability distribution for oil spill footprint backscatter $(\beta_{i,j})$ in raw and column of SAR data. If $(\beta_{i,j})$ is stated as the continuous oil spill backscatter variations that stick to the probability density function of $f(\beta_{i,j})$, the conditional entropy can be expressed in the form of conditional probability density function $f(\beta_1|\beta_2)$ of two given continuous random variants of radar backscatter (β_1) and (β_2). Thus the concept of conditional probability density function $f(\beta_1|\beta_2)$ [20] can be estimated by

$$E(\beta_1|\beta_2) = -\int_{-\infty}^{+\infty} \int_{-\infty}^{+\infty} f(\beta_1,\beta_2)\ln f((\beta_1|\beta_2)d\beta_1 d\beta_2 \tag{10}$$

where $d\beta_1 d\beta_2$ is the interval change of oil spill and look-alikes footprint backscatter, respectively.

Marghany [2], Staples and Rodrigues [11], Marghany and Genderen [12] and Lee [28] proved the efficiency and validity of the entropy on oil spill detection in SAR data. However, this approach requires range of threshold procedures to discriminate between oil spill footprint quantities and surrounding environment. Therefore, multiplicative speckle noise is not totally vanished. In this prospective, Multi-objective Optimization algorithm can involve in entropy metric [27] to preserve the diversity among different solution to minimize the influence of look-alikes and multiplicative speckle noise.

2.2.2 Entropy-Based Multi-objective Evolutionary Algorithm (E-MMGA)

E-MMGA provides the advantage of preserving the diversity of solution set [27] and solving the multidisciplinary of oil spill uncertainty of random oil spill footprint discrimination in SAR data. The approach of this study is to deal with entropy of oil spill detection as multi-objective Genetic Algorithm (GA). Following Coello et al. [21], multi-objective optimization (MOP) has already been successfully adopted into the engineering fields. In general, MOP consists of n decision variable parameters, k objective functions and m constraints [14]. Multi-objective Optimization [22, 27] aims at conducting optimization for a range of functions as follows [27]:

$$\text{Minimize } \vec{F} = (f_1(\beta), f_2(\beta),........, f_m(\beta))^T \tag{11}$$

$$\text{Subject to } E(\beta_1 | \beta_2) \in I \in \Omega \tag{12}$$

where I is SAR data and Ω is the definition domain of functions or the feasible region in space decision. In this research, two objectives are considered. One is oil spill backscatter and the other is sea surface, ship, lookalikes, and land backscatters. The definitions of entropy of oil spill and non- oil spill footprint boundaries are given as follows:

1. Entropy of oil spill footprint boundaries ($E(\beta_{max})$)is the variation of maximum entropy $E(\beta_{max})$ which contains oil spill footprint boundaries i.e. $E(\beta_{max}) = \max\{E(\beta_1, \beta_2,..., \beta_k)\}$; where $E(\beta_{ij})$ denotes the entropy of oil spill boundaries in i and j directions ij, $\forall ij = 1,2,...,k$.

2. The total entropy of oil spill footprint boundaries ($\sum E(\beta_{ij})$) is the sum of entropy of the surrounding oil spill environment in SAR data. Then the Pareto optimal solutions are applied to retain the discrimination of oil spills entropy diversity and surrounding entropy environment.

Let $E(\beta_0, \beta_1, \beta_2) \in E(\beta_{SAR})$, and $E(\beta_{SAR})$ is feasible entropy in the whole SAR image, while β_0 is called the Pareto optimal solution in the minimization problem for identification of oil spill pixels. If the following conditions are satisfied [22]:

(i)　　If $f(E(\beta_1))$ is said to be partially greater than $f(E(\beta_2))$, i.e. $f_i(E(\beta_1)) \geq f_i(E(\beta_2)), \forall i = 1, 2,..., n$ and $f_i(E(\beta_1)) > f_i(E(\beta_2)), \exists i = 1, 2,..., n$,

then $E(\beta_1)$ is said to be dominated by ($E(\beta_2)$.

(ii)　　If there is no $E(\beta) \in E(\beta_{SAR})$ s.t. $E(\beta)$ dominates $E(\beta_0)$, then $E(\beta_0)$ is the Pareto optimal solutions for identifying entropy of oil spill footprint boundaries $E(\beta_{max})$.

Following Marghany [22, 24], the optimization of oil spill detection from SAR data using entropy based MOEA E-MOEA, the entropy of oil spill footprint boundaries must be coded into a Genetic Algorithm syntax form i.e. the chromosome form. In this problem, the chromosome consists of a number of genes where every gene corresponds to a coefficient in

the nth-order surface fitting polynomial as given by.

$$f(i,j) = E(\beta_0 + \beta_1 i + \beta_2 j + \beta_3 i^2 + \beta_4 ij + \beta_5 j^2 + \ldots + \beta_m j^n) \qquad (13)$$

where $E(\beta)[0,1\ldots..m]$ are the entropy parameter coefficients that will be estimated by the genetic algorithm to approximate the minimum error for entropy of oil spill discrimination from the surrounding environment. i and j are indices of the pixel location in the image respectively, m is the number of coefficients (Figure 2).

| $E(\beta_0)$ | $E(\beta_1)$ | $E(\beta_2)$ | $E(\beta_3)$ | $E(\beta_4)$ | .... | $E(\beta_m)$ |

Figure 2: Coding scheme of the coefficients of the nth-order surface fitting polynomial into the chromosome syntax form.

Then the weighed sum to combine entropy of multiple objectives into single objective is given by [24]

$$f(E(\beta)) = w_1 f_1(E(\beta)) + w_2 f_2(E(\beta)) + \cdots + w_n f_n((E\beta)) \qquad (14)$$

where $f_1(E(\beta)), f_2(E(\beta)), \ldots, f_n(E(\beta))$ are the objective functions and $W_1, W_2, \ldots, W_n$ are the weights of corresponding objectives that satisfy the following conditions.

$$w_i \geq 0 \quad \forall i = 1, 2, \ldots, n$$
$$w_1 + w_2 + \ldots\ldots + w_n = 1 \qquad (15)$$

Once the weights are determined, the searching direction is fixed. To search Pareto optimal solutions as much as possible, the searching directions should be changed again and again to sweep over the whole solution space. Therefore the weights have to be changed again and again. The weights consist of random numbers and they are generated as the following way [22]:

$$w_i = \frac{r_i}{r_1 + r_2 + \cdots + r_n}, \quad \forall i = 1, 2, \ldots, n \qquad (16)$$

where $r_1, r_2, \ldots, r_n$ are random numbers within (0,1). Solutions searched through the changing directions are collected in a set. Then the definition of Pareto optimal solution is applied to determine which solutions in the set are Pareto optimal. The step repeats in every generation in E-MOGA. To determine the diversity of entropy of multi-objectives which is mostly more than two objectives for instance, oil spill, look-alikes, rough sea, and low wind zone, compute the distance from a given footprint center to its nearest neighbouring boundaries. This can be computed by the following equation adopted from Zhou et al., [23]:

$$\Psi = \sum_{k=1}^{m} d(E(\beta_{ij}),\Omega) + \sum_{I \in \Omega} \left| d(I,\Omega) - \bar{d} \right| \times$$
$$\left[\sum_{k=1}^{m} d(E(\beta_{ij}),\Omega) + (\left| \Omega - m \right|)\bar{d} \right]^{-1} \tag{17}$$

There are m solutions $E(\beta_1),................,E(\beta_m)$ sorted by an objective in SAR space data, $d_1,............,d_{m-1}$ are the edge distances between adjacent different oil spill and look-alike footprint boundaries and Ω is set of solutions regarding oil spill or look-alikes footprint boundaries, and

$$d(E(\beta_1),\Omega) = \min_{E(\beta_j) \in \Omega, E(\beta_j) \neq E(\beta_i)} \left\| F(E(\beta_i)) - F(E(\beta_j)) \right\| \tag{18}$$

$$d = \left| \Omega \right|^{-1} \sum_{E(\beta) \in \Omega} d(E(\beta),\Omega). \tag{19}$$

E-MMGA is run until there is no further improvement in the entropy value (i.e., entropy is maximum), and then it is stopped. The solution of the overall problem is obtained by taking the non-dominated frontier of the points in the grand pool of the last E-MMGA iteration.

3.0 RESULTS AND DISCUSSION

The Entropy and E-MMGA are trained on four RADARSAT-2 SAR Scan Narrow Beam (SCNB) data, whereas the dark spots were identified and examined. The Scan Narrow Beam (SCNB) images contained the confirmed oil spills that occurred 70 km from the coast of Louisiana in the Gulf of Mexico. In the RADARSAT-2 SAR Scan Narrow Beam (SCNB) data that were acquired at the time, the rapid growth of the oil slick footprint from April 27, 2010 to May 5, 2010 could be clearly seen (Fig. 3a). Figure 3b shows that crude oil extended across 19,112 square miles (49,500 km^2) of the Gulf. Additionally, it is precious to note that the oil slick spun in a counter-clockwise direction due to the influence of the loop current of Gulf Stream. Nevertheless, the RADARSAT-2 SAR data did not indicate that the oil-slick footprint coincided with the loop current in the Gulf of Mexico. In fact, the oil slick was one due to the disconnection of the loop current in the Gulf of Mexico [24]. Furthermore, Figure 3 shows the variation in the average backscatter intensity along the oil slick footprint. The average backscatter intensity was damped by -30 dB to -5 dB and decreased over time as the oil slick footprint gradually increased (Figure 4). Besides, the sea surface roughness has the highest backscatter values of -10 dB than oil spill footprint pixels.

Consistent with Marghany [25] and Trivero et al., [25], oil spills change the roughness of the ocean surface to smoothness surface which appear as dark pixels as compared to the surrounding ocean [1, 3, 8]. Consequently, the speckle caused obstacles in dark patch identifications in SAR data [12-14]. Additionally, the wind speed recorded on April 27 2010 was ranged between 7 to 10 m/s [24]. Besides, the measured reductions of backscattered radar power at C-band could be impacted by instrumental limitations, i.e. by the fact that the backscattered radar power reaches the noise floor [25].
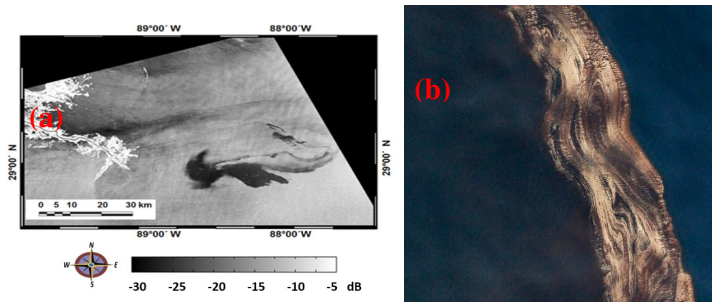
Figure 3: RADARSAT-2 SAR Scan Narrow beam SCNB data in (a) April 27th, and (b) in situ crude oil.

Figure 4 shows the entropy algorithm result. Clearly, the oil spill footprint has lower entropy value of 1.5 as compared to sea roughness and land. The land has the highest entropy value of 3.5 and sea roughness has entropy value of 2.7. Indeed, non-Bragg scattering exists on land as backscatter becomes depolarized [1, 25]. Additionally, entropy algorithm has identified oil spill footprint boundaries by entropy value of 3.3. However, land entropy and oil spill footprint boundary have close entropy. In fact, entropy represents the randomness of scattering mechanism. According to Marghany [2] entropy is a measure of uniformity in SAR image. In general, the entropy is a measure of variability or randomness because the concentration of the backscatter changes in relatively few locations would be non-random essentially.
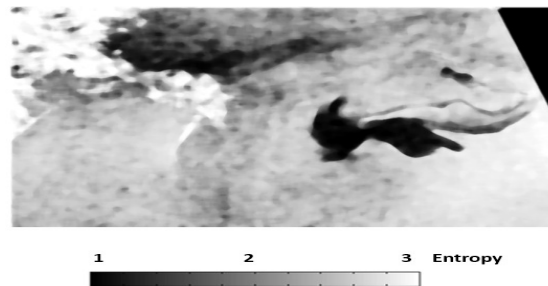
Figure 4: Entropy result for oil spill footprint.

Figure 5 shows the output result of E-MMGA. Clearly, E-MMGA is able to produce four different segmentation boundaries. Besides, Figure 6 shows that the thick oil spill footprint has the highest E-MMGA value of 2 than medium and light oil spill. This is mainly because each multi-objective function in E-MMGA tends to bias its population towards the extreme edges of the Pareto frontier. This confirms the work done by Gunawan et al. [27]. Compared to entropy algorithm, E-MMGA is able to identify the look-alike footprint boundaries and discriminate accurately between, oil spill and look-alikes, and surrounding sea surface. E-MMGA can accurately identify the morphological boundary of oil spill and is assigned by different segmentation layer in Scan Narrow beam SCNB data satellite. In fact, the Entropy-Multi-Objective Evolutionary Genetic Algorithm (E-MMGA) provides a set of compromised solutions called Pareto optimal solution since no single solution can optimize each of the

objectives separately. The decision maker is provided with the set of Pareto optimal solutions in order to choose solution based on the decision maker's criteria. This sort of E-MMGA solution technique is called a posteriori method since decision is taken after searching is finished. This confirms the work done by Coello et al. [21]. In this context, the Pareto-optimization approach does not require any a priori preference decisions between the conflicting of oil spill, look-alike, land, and surrounding sea footprint boundaries. Furthermore, Pareto-optimal points have form Pareto-front as shown in Figure 6 in the multi-objectives function of the Scan Narrow beam SCNB data.

Figure 5: E-MMGA solution for oil spill discrimination in Scan Narrow beam SCNB data.
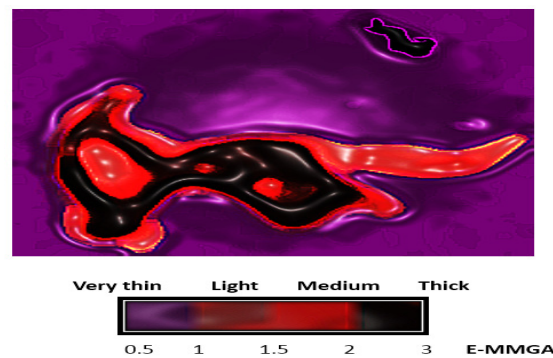
Figure 6: Oil spill footprint Category by E-MMGA.

Entropy-Multi-Objectives Evaluation Genetic Algorithm (E-MMGA) which is based on the Pareto optimal solutions provides excellent discrimination of oil spill footprint boundaries. This can be confirmed by the receiver–operator characteristics (ROC) curve (Fig. 7). In this regard, the existing of weight sum of objective function converts a conflicting multi-objective problem of oil spill and surrounding sea feature objectives. This can be seen in ROC curve where oil spill has an area difference of 85% which is larger than look-alike and sea surface areas. Furthermore, p probability of 0.0005 is another proof for excellent of E-MMGA for oil spill detection. This study shows a great performance as compared to previous work done by Marghany [22, 24]. This is because Pareto-front contains the Pareto-optimal solutions and in the case of continuous front, it divides the pixels objective function space into two parts, which are non-optimal solutions and infeasible solutions. In this regard, it improves the robustness of pattern search and improves the convergence speed of MOEA. This confirms the work of Yudong et al., [26].
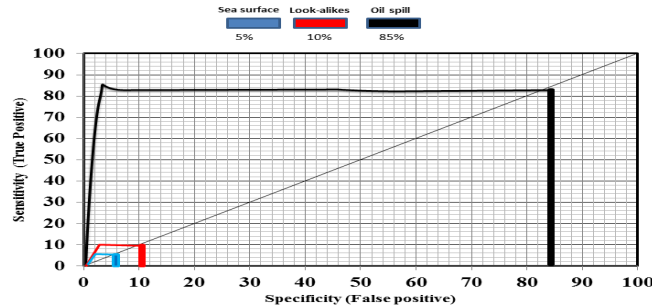
Figure 7: ROC for oil spill discrimination using E-MMGA.

On the word of Gunawan et al. [27], E-MMGA is able to preserve diversity and converge as fast as most of the single-level approaches (which are expected to be more efficient but less practical for large-scale problems of multidisciplinary nature). Besides, it improves overall quality of solutions by explicitly optimizing the entropy index at every system-level iteration, and then using this information to make the search process bias towards obtaining a solution set with maximum diversity [27].

4.0 CONCLUSSION

This study has demonstrated work to optimize the oil spill footprint detection in synthetic aperture radar (SAR) data. Therefore, Entropy-based Multi-objective Evolutionary Algorithm (E-MMGA) was implemented with Scan Narrow beam SCNB data satellite during the oil spill event along the coastal water Gulf of Mexico. Besides, Pareto optimal solution is implemented with E-MMGA to minimize the difficulties of oil spill footprint boundary detection because of the existence of look-alike in SAR data. The study shows that the implementation of Pareto optimal solution and weight sum in E-MMGA generated accurate pattern of oil slick. Furthermore, thick oil spill has the highest value of 2 E-MMGA than thin and medium spills. The E-MMGA is able to preserve the morphology of oil spill footprint boundaries i.e. thick, medium, and light. In addition, the receiver –operational characteristics (ROC) curve confirmed accurately the performance of E-MMGA with 85% oil spill detection, 10% for look-alike and 5% for surrounding sea surface boundary identification. In conclusion, E-MMGA is considered as an excellent algorithm to discriminate oil spill from look-alikes and also to identify thick oil spill from thin one.

ACKNOWLEDGEMENT

REFERENCES

[1]   P.P. Lombardini, B. Fiscella, P. Trivero, C. Cappa, W.D. Garrett, Modulation of the spectra of short gravity waves by sea surface films: slick detection and characterization with microwave probe, Journal of Atmospheric and Oceanic Technology 6 (1989) 882-890.

[2]   M. Marghany, RADARSAT automatic algorithms for detecting coastal oil spill pollution, International Journal of Applied Earth Observation and Geoinformation 3 (2001) 191-196.

[3]   K. Fukunaga, Introduction to statistical pattern recognition, 2ND Ed., Academic Press, New York, USA (1990).

[4]   P. Teivero, B. Fiscella, F. Gomez, P. Pavese, SAR detection and characterisation of sea surface slicks, International Journal of Remote Sensing 19 (1998) 543-548.

[5]   I.S. Mohamed, A.M. Salleh, L.C. Tze, Detection of oil spills in Malaysian waters from RADARSAT Synthetic Aperture Radar data and prediction of oil spill movement, Proceeding of 19th Asian Conference on Remote Sensing, China, Hong Kong, 23-27, November 1999, Asian Remote Sensing Society, Japan 2 (1999) 980-987.

[6]   G. Calaberesi, F. Del Frate, J. Lightenegger, A. Petrocchi, P. Trivero, Neural networks for the oil spill detection using ERS-SAR data, In Proceedings of Geoscience and Remote Sensing Symposium, 1999, IGARSS'99, Hamburg, Germany, 28 June 2 July 1999, IEEE Geoscience and Remote Sensing Society, USA 1 (1999) 215-217.

[7]   L.Z. Shi, C. Fan, K. Shi, L. Peng, Texture feature application in oil spill detection by satellite data, Proceedings of Image and Signal Processing, CISP, Sanya, China 27-30 May (2008) 784-788.

[8]   S. Skrunes, C. Brekke, T. Eltoft, An Experimental study on oil spill Characterization by Multi-Polarization SAR, in Proceedings of European conference on Synthetic Aperture Radar, Nuremberg, Germany (2012) 139-142.

[9]   B. Minchew, C. Jones, B. Holt, Polarimetric Analysis of Backscatter From the Deepwater Horizon Oil Spill Using L-Band Synthetic Aperture Radar, IEEE Transaction on Geoscience Remote Sensing 10 (2012) 123-139.

[10] S.R. Cloude, E. Pottier, A review of target decomposition theorems in radar polarimetry, IEEE Transactions on Geoscience and Remote Sensing 34 (1996) 498-518.

[11] G. Staples, D.F. Rodrigues, Maritime environmental surveillance with RADARSAT 2, Anais XVI Simpósio Brasileiro de Sensoriamento Remoto - SBSR, Foz do Iguaçu, PR, Brasil, 13 a 18 de abril de, INPE (2013).

[12] M. Marghany, J. Genderen, Entropy algorithm for automatic detection of oil spill from radarsat-2 SAR data, 8th International Symposium of the Digital Earth (ISDE8), IOP Conf. Series: Earth and Environmental Science 18 (2014) 012051.

[13] K. Topouzelis, D. Stathakis, V. Karathanassi, Investigation of genetic algorithms contribution to feature selection for oil spill detection, International Journal of Remote Sensing 30 (2009) 611-625.

[14] M. Marghany, B. Murgante, S. Misra, M. Carlini, C.M. Torre, H. Nguyen, D. Taniar, B.O. Apduhan, O. Gervasi, Genetic algorithm for oil spill automatic detection from envisat satellite data, Computational Science and Its Applications – ICCSA 7972 (2013) 587-598.

[15] R.K. Mohanta, B. Sethi, A review of genetic algorithm application for image segmentation, International Journal of Computer Technology & Applications 3 (2011) 720-723.

[16] O. Garcia-Pineda, I.R. MacDonald, X. Li, C.R. Jackson, W.G. Pichel, oil spill mapping and measurement in the gulf of mexico with textural classifier neural network algorithm (tcnna), Selected Topics in Applied Earth Observations and Remote Sensing 99 (2013) 1-9.

[17] N.B. Harmancioglu, Measuring the information content of hydrological processes by the entropy concept, Journal of Civil Engineering (1981) 13-38.

[18] B.P. Lati, An introduction to random signals and communication theory; International Textbook Company, Scranton, Pennsylvania (1968).

[19] J. Amorocho, B. Espildora, Entropy in the assessment of uncertainty in hydrologic systems and models, Water Resour. Res. 9 (1973) 1511-1522.

[20] T.G. Chapman, Entropy as a measure of hydrologic data uncertainty and model performance, Journal of Hydrology 86 (1986) 111-126.

[21] C.A. Coello, G.B. Lamont, D. Veldhuizen, Evolutionary algorithms for solving multi-objective problems, 2nd Edition, Springer, Berlin, (2007).

[22] M. Marghany, B. Murgante, S. Misra, M. Carlini, M.C. Torre, H. Nguyen, D. Taniar, B. Apduhan, O. Gervasi, Multi-objective evolutionary algorithm for oil spill detection from COSMO-SkeyMed satellite, ICCSA 2014, Part VI (2014) 355-371.

[23] A. Zhou, Y. Jin, Q. Zhang, B. Sendhoff, E. Tsang, Combining model-based and genetics-based offspring generation for multi-objective optimization using a convergence criterion, in Proceedings of the IEEE Congress on Evolutionary Computation (CEC '06), pp. 3234–3240, July (2006).

[24] M. Marghany, Utilization of a genetic algorithm for the automatic detection of oil spill from RADARSAT-2 SAR satellite data, Marine Pollution Bulletin 89 (2014) 20-29.

[25] P. Trivero, F. Nirchio, High resolution COSMO - SkyMed SAR images for oil spills automatic detection, Geoscience and Remote Sensing Symposium, IEEE International IGARSS (2007) 2-5.

[26] Z. Yudong, W Shuihua, J. Genlin, D. Zhengchao. Genetic Pattern Search and Its Application to Brain Image Classification, Mathematical Problem in Engineering (2013) 1-8.

[27] S. Gunawan, A. Farhang-Mehr, S. Azarm, On maximizing solution diversity in a multiobjective multidisciplinary genetic algorithm for design optimization, Mechanics Based Design of Structures and Machines: An International Journal 32 (2004) 491-514.

[28] J. Lee, Determination of optimal water quality monitoring points in sewer systems using entropy theory, Entropy 15 (2013) 3419-3434.